Electrochemistry Hot Paper

International Edition: DOI: 10.1002/anie.201509008
German Edition: DOI: 10.1002/ange.201509008

The Electrochemical Characterization of Single Core–Shell Nanoparticles

Lucy R. Holt[+], Blake J. Plowman[+], Neil P. Young, Kristina Tschulik, and Richard G. Compton**

Abstract: *We report the direct solution-phase characterization of individual gold-core silver-shell nanoparticles through an electrochemical means, with selectivity achieved between the core and shell components based on their different redox activities. The electrochemically determined core–shell sizes are in excellent agreement with electron microscopy-based results, successfully demonstrating the electrochemical characterization of individual core–shell nanoparticles.*

As interest in the behavior of nanoparticles has continued to increase, many research efforts have been devoted to novel ways to fabricate, characterize and explore their fascinating properties.[1] This includes studies directed towards the size, shape, composition, and functionalization of the particles, leading to sophisticated nanomaterials specifically designed for their intended applications. One such exciting development is the fabrication of core–shell nanoparticles, which have been found to possess novel optical, catalytic, magnetic, and sensing properties, to name a few.[2] However a remaining challenge in this area lies in the difficulty of obtaining rapid, quantitative characterization of the core–shell nanomaterials. Techniques such as transmission electron microscopy (TEM), dynamic light scattering (DLS), and optical spectroscopy are well suited for the routine characterization of single-component nanoparticles. These studies have also been extended to individual nanoparticles, as illustrated by in situ TEM imaging of lithium battery materials[3] and by optical-electrochemical 3D microscopy of single silver nanoparticles.[4] However determining the dimensions of core–shell nanoparticles through such methods can entail a number of limitations. For example DLS and optical spectroscopy generally provide indirect evidence of the core–shell dimensions and may require materials with a suitable surface plasmon resonance, and while TEM imaging may provide in situ characterization[3a,5] it is routinely used to provide ex situ data which may be susceptible to poor elemental contrast, low sample throughput or contamination from other species present in the nanoparticle suspension.[2a,6] Herein we therefore explore for the first time the electrochemical characterization of individual core–shell nanoparticles. This approach is through the use of nanoimpact experiments, where the Brownian motion driven collision of a nanoparticle with an electrode enables its in situ characterization by monitoring the charge transfer between this single nanoparticle and the electrode surface.[7] This powerful strategy has been successfully demonstrated for a wide range of metallic, organic, and inorganic nanostructures, shedding light on their size, shape, and reactivity,[8] however it has not yet been exploited for bimetallic nanoparticles. For this purpose the gold-core silver-shell system is chosen, given that it is one of the most widely studied bimetallic core–shell systems[9] because of its favorable properties for a number of state-of-the-art technologies such as surface-enhanced Raman spectroscopy (SERS), surface plasmon resonance (SPR) sensing and antibacterial applications.[10] This system therefore provides an attractive framework to explore a direct electrochemical probe for the characterization of individual core–shell nanoparticles.

In order to quantitatively analyze the gold-core silver-shell nanoparticles the electrochemical behavior of cetyl trimethylammonium bromide (CTAB) capped gold nanoparticles was first established. This was necessitated as the electrochemical dissolution of gold can take place by two processes [Eqs. (1),(2)],[11] so by determining the effective number of electrons transferred during the dissolution of gold the results from the core–shell nanoparticles can be rationalized.

$$Au + 2\,Cl^- \rightleftharpoons AuCl_2^- + e^- \quad (1)$$

$$Au + 4\,Cl^- \rightleftharpoons AuCl_4^- + 3\,e^- \quad (2)$$

As can be seen from the TEM image in Figure 1a, the CTAB-capped gold nanoparticles are quasi-spherical in shape, with a mean diameter of 25.2 ± 0.4 nm. The electrochemical behavior of the gold nanoparticles was first investigated by cyclic voltammetry (CV) using a drop cast modified glassy carbon electrode (Figure 1b). Note that the voltammetry was performed in 20 mM HCl in order to provide a low ionic strength for nanoimpact experiments, with the presence of Cl^- aiding the dissolution of gold[11–12] and inhibiting the O_2-driven dissolution of silver in the case of the core–shell

[*] L. R. Holt,[+] Dr. B. J. Plowman,[+] Dr. K. Tschulik, Prof. R. G. Compton
Department of Chemistry
Physical and Theoretical Chemistry Laboratory
University of Oxford, South Parks Road
Oxford, OX13QZ (UK)
E-mail: kristina.tschulik@rub.de
richard.compton@chem.ox.ac.uk
Dr. N. P. Young
Department of Materials, University of Oxford
Parks Road, OX13PH (UK)
Dr. K. Tschulik
Nano-Electrochemistry-Center for Electrochemical Sciences
Faculty of Chemistry and Biochemistry
Ruhr-University Bochum
44780 Bochum (Germany)
[+] These authors contributed equally to this work.

Supporting information for this article is available on the WWW under http://dx.doi.org/10.1002/anie.201509008.

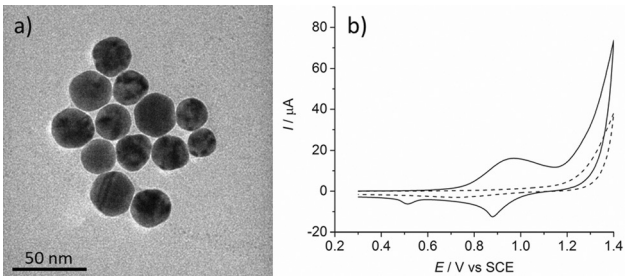

Figure 1. a) Bright-field TEM image of the gold nanoparticles. b) Cyclic voltammograms of a glassy carbon substrate in 20 mM HCl at 25 mVs^{-1} before (dashed line) and after modification with 4 μL of gold nanoparticles (solid line).

nanoparticles.[13] As can be seen in Figure 1b, a broad oxidative peak is apparent at 0.97 V which is attributed to both the dissolution of gold [Eqs. (1),(2)][11] and the oxidation of Br^- which may then react to form tribromide [Eqs. (3), (4)].[14] On the reverse scan the reduction of Br_2 to Br^- is seen (0.88 V) as well as the reduction of the $AuCl_x^-$ species formed in the forward scan (0.51 V).

$$2\,Br^- \rightleftharpoons Br_2 + 2\,e^- \quad (3)$$

$$Br_2 + Br^- \rightleftharpoons Br_3^- \quad (4)$$

Because of the overlap between the gold and bromide oxidation processes the charge relating to the broad anodic peak at 0.97 V was not used to determine the reaction pathway for the dissolution of the gold nanoparticles. For this purpose nanoimpact experiments were performed using a 1 pM gold nanoparticle suspension in 20 mM HCl with a microcylinder electrode.[15] While current spikes were not observed in the absence of gold nanoparticles (see Figure S1 in the Supporting Information) or at potentials where gold dissolution is not expected (Figure S2) based on the cyclic voltammogram in Figure 1a, well-resolved spikes were clearly observed at more oxidizing potentials (Figure 2a). These spikes show a distribution of sizes, reflecting the size distribution of the nanoparticles present. Experiments were therefore performed at potentials between 0.7 V to 1.5 V, with the mean oxidative charges obtained (and the standard error of the mean) from 538 impacts (at an average of 67 impacts for each potential studied) shown in Figure 2b. As can be seen

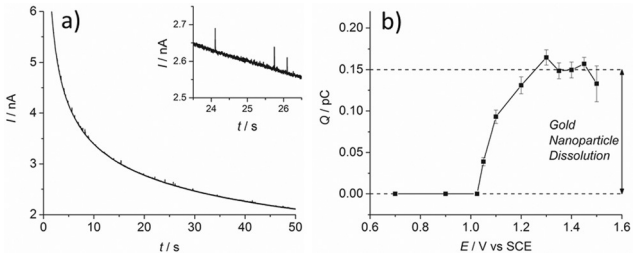

Figure 2. a) Chronoamperogram recorded at a carbon fiber microcylinder electrode at 1.3 V in 20 mM HCl with 1 pM gold nanoparticles. b) The potential dependency of the oxidative impacts of the gold nanoparticles.

no impacts were observed for the lower potentials studied, however spikes were detected at a potential of 1.05 V, indicating the onset of gold dissolution. At higher potentials this oxidative charge is seen to increase until a plateau is reached at approximately 0.15 pC, marking the complete dissolution of the gold nanoparticles.

Having established the mean oxidative charge for the dissolution of the gold nanoparticles, the average number of electrons transferred for the oxidation of each gold atom was then determined. This was achieved by calculating the average number of gold atoms present in the 25.2 nm diameter particles (as measured by TEM), which gave an average of ca. 8.2×10^{-19} moles of gold per nanoparticle. By relating this number with the average oxidation charge, the effective number of electrons involved in the dissolution of gold is found to be 1.9, in agreement with previous work on citrate-capped gold nanoparticles.[16] This indicates that the dissolution of the gold nanoparticles proceeds the formation of both Au^I [Eq. (1)] and Au^{III} species [Eq. (2)], and importantly this value provides a means to rationalize the observed charge in the case of the core–shell nanoparticles.

To determine the dimensions of the core–shell nanoparticles TEM image analysis was performed, and as can be seen from the bright field image in Figure 3a the core–shell

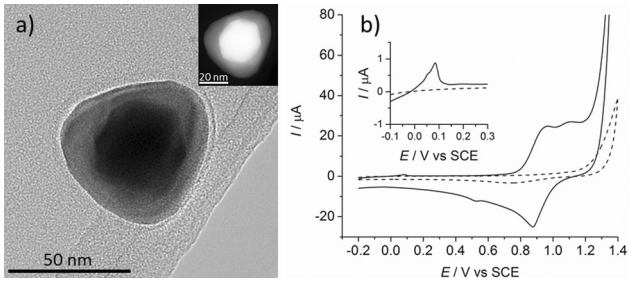

Figure 3. a) Bright-field TEM image of a gold-core silver-shell nanoparticle along with a HAADF-STEM image (inset). b) Cyclic voltammograms recorded at 25 mVs^{-1} in 20 mM HCl with a glassy carbon electrode before (dashed line) and after modification with 20 μL of gold-core silver-shell nanoparticles (solid line).

configuration of the nanoparticles is evident. Imaging was also obtained using high angle annular dark field scanning transmission electron microscopy (HAADF-STEM) mode, owing to its improved atomic number contrast,[17] and as shown in the inset of Figure 3a this allowed a clear distinction to be made between the gold cores and the silver shells. Analysis of the TEM images showed an average gold core diameter of 29.6 ± 1.1 nm with a silver shell thickness of 6.1 ± 0.7 nm.

The electrochemical response of the core–shell nanoparticles was then determined in 20 mM HCl (Figure 3b). Here the oxidation of silver can be observed at 0.08 V, in agreement with previous work,[18] followed by a broad oxidation attributed to the dissolution of gold and the oxidation of bromide (0.97 V). On the reverse scan the subsequent reduction of Br_2 occurs at 0.88 V, after which the reduction of gold species formed during the forward scan

takes place at 0.53 V, as confirmed by comparison with Figure 1b as well as previous work.[16]

Nanoimpact experiments were then performed to demonstrate the quantitative analysis of single bimetallic core–shell nanoparticles. As expected, no spikes were observed in the control experiments run at a high oxidizing potential (1.3 V) in the absence of nanoparticles (Figure S1) or at a potential of 0.6 V in the presence of the nanoparticles (Figure S3). However clear spikes were obtained in the presence of the core–shell nanoparticles when the potential was raised to 0.9 V (Figure 4a). As no spikes had been

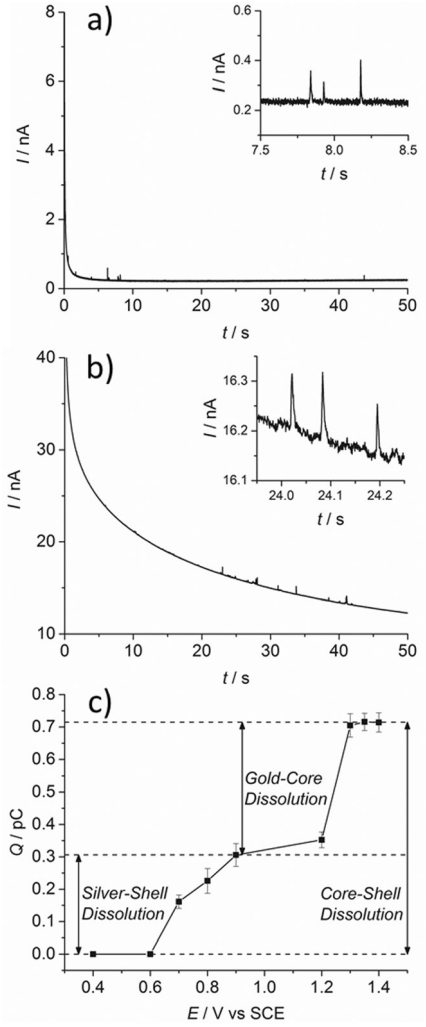

Figure 4. Chronoamperograms recorded at a carbon microcylinder electrode at a) 0.9 V or b) 1.3 V in a solution of 20 mM HCl with 0.1 pM gold-core silver-shell nanoparticles. c) The potential dependency of the oxidative impacts of the gold-core silver-shell nanoparticles.

observed at this potential in the case of the monometallic gold nanoparticles (Figure 2b), this is therefore attributed to the oxidation of the silver shells. Upon increasing the applied potential to 1.3 V (where the dissolution of the gold nanoparticles had been apparent), larger spikes were observed than the ones recorded at 0.9 V (Figure 4b). This is due to the combined dissolution of both the silver shells and the gold cores.

A potential dependent study of these processes was then conducted, with the results of 442 impacts (at an average of 63 impacts for each potential studied) presented in Figure 4c. This shows the onset of silver oxidation at 0.7 V, with the charge increasing with the applied potential until a value of approximately 0.3 pC. A further step in the charge is then apparent above 1.2 V, where the charge reaches a plateau at approximately 0.7 pC. As this value corresponds to the complete dissolution of the core–shell nanoparticles, the oxidative charge associated with the gold core dissolution is therefore approximately 0.4 pC. To confirm the quantitative nature of this analysis the average diameter of the gold cores was then determined by utilizing a 1.9 electron oxidation per gold atom (as established earlier) and assuming the particles are spherical in nature. This leads to a gold core diameter of 35.1 ± 0.9 nm, and by calculating the thickness of a silver shell on a core of this size given a charge of 0.3 pC this leads to an average shell thickness of 6.1 ± 0.5 nm. As can be seen excellent agreement is obtained between the nanoimpact experiments and the TEM analysis, as the differences may be accounted for by errors in estimating the volume of the nanoparticles from the 2D TEM images.

In this Communication we have successfully demonstrated the quantitative characterization of individual core–shell nanoparticles through electrochemical nanoimpact experiments. This strategy provides a unique and powerful approach to obtain accurate in situ characterization of multicomponent nanoparticles with more noble core materials, and may be especially beneficial for cases where electron microscopy of the core and shell materials show limited contrast differences. As full characterization requires analysis at different potentials it should be noted that this analysis cannot be performed on the same impacting nanoparticle. Nevertheless the method provides further promise as a fast screening method which lacks the sample preparation requirements of other characterization techniques. While such analysis has been established in the case of the gold-core silver-shell system, which is recognized as one of the most widely studied core–shell systems, this approach can readily be extended to a host of other core–shell structures, opening up a new method to characterize a wide range of bimetallic nanoparticles.

Acknowledgements

The authors gratefully acknowledge the support of this work through a Marie Curie International Incoming Fellowship (B.J.P., project number 630069), the Ministry of Innovation, Science and Research of the State of North Rhine-Westphalia (Rückkehrerprogramm), the Cluster of Excellence RESOLV (EXC 1069) funded by the German Research Foundation (DFG) (K.T.) and a Royal Society of Chemistry Undergraduate Research Bursary (L.H.).

Keywords: analytical chemistry · bimetallic · core–shell nanoparticles · electrochemistry · surface chemistry

How to cite: *Angew. Chem. Int. Ed.* **2016**, *55*, 397 – 400
Angew. Chem. **2016**, *128*, 405 – 408

[1] a) M. L. Personick, C. A. Mirkin, *J. Am. Chem. Soc.* **2013**, *135*, 18238 – 18247; b) Y. Xia, Y. Xiong, B. Lim, S. E. Skrabalak, *Angew. Chem. Int. Ed.* **2009**, *48*, 60 – 103; *Angew. Chem.* **2009**, *121*, 62 – 108.
[2] a) R. Ghosh Chaudhuri, S. Paria, *Chem. Rev.* **2011**, *111*, 2373 – 2433; b) C.-J. Zhong, M. M. Maye, *Adv. Mater.* **2001**, *13*, 1507 – 1511.
[3] a) X. H. Liu, J. Y. Huang, *Energy Environ. Sci.* **2011**, *4*, 3844 – 3860; b) X. H. Liu, L. Zhong, S. Huang, S. X. Mao, T. Zhu, J. Y. Huang, *ACS Nano* **2012**, *6*, 1522 – 1531.
[4] A. N. Patel, A. Martinez-Marrades, V. Brasiliense, D. Koshelev, M. Besbes, R. Kuszelewicz, C. Combellas, G. Tessier, F. Kanoufi, *Nano Lett.* **2015**, *0*, 0.
[5] a) S. B. Simonsen, I. Chorkendorff, S. Dahl, M. Skoglundh, J. Sehested, S. Helveg, *J. Am. Chem. Soc.* **2010**, *132*, 7968 – 7975; b) J. Wu, W. Gao, J. Wen, D. J. Miller, P. Lu, J.-M. Zuo, H. Yang, *Nano Lett.* **2015**, *15*, 2711 – 2715.
[6] a) D. R. Baer, J. E. Amonette, M. H. Engelhard, D. J. Gaspar, A. S. Karakoti, S. Kuchibhatla, P. Nachimuthu, J. Nurmi, Y. Qiang, V. Sarathy, *Surf. Interface Anal.* **2008**, *40*, 529 – 537; b) E. J. Cho, H. Holback, K. C. Liu, S. A. Abouelmagd, J. Park, Y. Yeo, *Mol. Pharm.* **2013**, *10*, 2093 – 2110; c) M. Gaumet, A. Vargas, R. Gurny, F. Delie, *Eur. J. Pharm. Biopharm.* **2008**, *69*, 1 – 9.
[7] M. Pumera, *ACS Nano* **2014**, *8*, 7555 – 7558.
[8] a) T. R. Bartlett, S. V. Sokolov, R. G. Compton, *ChemistryOpen* **2015**, *4*, 600 – 605; b) W. Cheng, R. G. Compton, *TRAC Trends Anal. Chem.* **2014**, *58*, 79 – 89; c) W. Cheng, R. G. Compton, *Angew. Chem. Int. Ed.* **2014**, *53*, 13928 – 13930; *Angew. Chem.* **2014**, *126*, 14148 – 14150; d) W. Cheng, X. F. Zhou, R. G. Compton, *Angew. Chem. Int. Ed.* **2013**, *52*, 12980 – 12982; *Angew. Chem.* **2013**, *125*, 13218 – 13220; e) Y.-G. Zhou, N. V. Rees, R. G. Compton, *Angew. Chem. Int. Ed.* **2011**, *50*, 4219 – 4221; *Angew. Chem.* **2011**, *123*, 4305 – 4307.
[9] H.-L. Jiang, T. Akita, T. Ishida, M. Haruta, Q. Xu, *J. Am. Chem. Soc.* **2011**, *133*, 1304 – 1306.
[10] a) M. Banerjee, S. Sharma, A. Chattopadhyay, S. S. Ghosh, *Nanoscale* **2011**, *3*, 5120 – 5125; b) L. Lu, H. Wang, Y. Zhou, S. Xi, H. Zhang, J. Hu, B. Zhao, *Chem. Commun.* **2002**, 144 – 145; c) A. Steinbrück, O. Stranik, A. Csaki, W. Fritzsche, *Anal. Bioanal. Chem.* **2011**, *401*, 1241 – 1249.
[11] Y. Zu, A. J. Bard, *Anal. Chem.* **2000**, *72*, 3223 – 3232.
[12] a) J. Wang, Y. Shao, Y. Jin, F. Wang, S. Dong, *Anal. Chem.* **2005**, *77*, 5760 – 5765; b) M. Pumera, M. Aldavert, C. Mills, A. Merkoçi, S. Alegret, *Electrochim. Acta* **2005**, *50*, 3702 – 3707.
[13] B. J. Plowman, K. Tschulik, E. Walport, N. P. Young, R. G. Compton, *Nanoscale* **2015**, *7*, 12361 – 12364.
[14] a) P. K. Adanuvor, R. E. White, S. E. Lorimer, *J. Electrochem. Soc.* **1987**, *134*, 1450 – 1454; b) G. D. Simpson, R. E. White, *J. Electrochem. Soc.* **1990**, *137*, 1843 – 1846.
[15] J. Ellison, C. Batchelor-McAuley, K. Tschulik, R. G. Compton, *Sens. Actuators B* **2014**, *200*, 47 – 52.
[16] Y.-G. Zhou, N. V. Rees, J. Pillay, R. Tshikhudo, S. Vilakazi, R. G. Compton, *Chem. Commun.* **2012**, *48*, 224 – 226.
[17] S. I. Sanchez, M. W. Small, J.-M. Zuo, R. G. Nuzzo, *J. Am. Chem. Soc.* **2009**, *131*, 8683 – 8689.
[18] M. Gulppi, J. Pavez, J. H. Zagal, M. Sancy, M. Azocar, F. Scholz, M. A. Páez, *J. Electroanal. Chem.* **2015**, *745*, 61 – 65.

Received: September 25, 2015
Revised: October 14, 2015
Published online: November 17, 2015

